

PHOTOCATALYTIC SELECTIVE OXIDATION OF ORGANIC COMPOUNDS IN GRAPHITIC CARBON NITRIDE SYSTEMS (Review)

UDC 544.525.6; 544.526:542.943

A. L. Stroyuk^{1,2*}, A. E. Raevskaya¹, and S. Ya. Kuchmy^{1†}

¹L. V. Pysarzhevsky Institute of Physical Chemistry, National Academy of Sciences of Ukraine, Prospekt Nauky 31, 03028 Kiev, Ukraine and ²Forschungszentrum Jülich GmbH, Helmholtz-Institut Erlangen Nürnberg für Erneuerbare Energien (HI ERN), Immerwahrstr. 2, 91058 Erlangen, Germany. Translated from *Teoreticheskaya i Éksperimental'naya Khimiya*, Vol. 55, No. 3, pp. 135-160, May-June, 2019. Original article submitted June 12, 2019.

*To whom correspondence should be addressed. E-mail: o.stroyuk@fz-juelich.de.

†To whom correspondence should be addressed. E-mail: kuchmiy@inphyschem-nas.kiev.ua.

Recent work is reviewed concerning photocatalytic systems derived from graphitic carbon nitride (GCN) for the selective oxidation of various organic compounds including saturated and unsaturated hydrocarbons, alcohols, and organic sulfides. Examples are given for oxidative coupling of a series of organic compounds with the formation of carbon–nitrogen and carbon–carbon bonds as well as cyclization. The properties of various GCN samples were examined, including bulk, mesoporous, layered, and individual materials as well as samples modified with organic compounds, samples doped with metals and nonmetals, and GCN-derived composite materials. The outlook for future research in this field is given at the conclusion.

Key words: graphitic carbon nitride, organic compounds, photocatalysis, oxidation, oxidative coupling, cyclization reactions.

Pioneering work by various groups [1-6] has demonstrated the feasibility of using graphitic carbon nitride (GCN or g-C₃N₄) as a photocatalyst and led to unflagging interest in this material during the past decade due to a number of attractive features of g-C₃N₄ such as partial absorption of visible light, band gap width (E_g) dependent on the method of synthesis and modification ranging from 1.9 to 2.7 eV, and potentials of the conductance band (E_{CB} , from -0.75 to -1.53 V relative to the normal hydrogen electrode (NHE)) and valence band (E_{VB} , from 1.03 to 1.9 V relative to NHE) (pH 7) [5, 7-19]. Such an arrangement of the energy levels of the photogenerated charge carriers permits g-C₃N₄ to induce both oxidative and reductive transformations of a broad range of substrates. In addition, this layered material has thermal and chemical stability and can be readily obtained by the pyrolysis of relatively inexpensive precursor compounds. These unique properties of g-C₃N₄ create the preconditions for its use as a component of both catalysts for various thermal reactions [5, 6, 10, 14, 17] and photocatalytic

systems, in particular, for the generation of hydrogen from aqueous solutions of electron-donor substrates and the complete dissociation of water [7-10, 12, 14, 16-26], water purification to remove organic and inorganic pollutants [7, 8, 12, 20-23], reduction of CO₂ [8, 12, 20-23, 27-32], electrical energy systems [11, 14, 22, 26, 33-36], as well as in organic synthesis [10, 11, 20, 23, 37-42].

Bulk graphitic carbon nitride is the product of the thermal polycondensation of nitrogen-rich compounds such as melamine, urea, cyanamide, dicyandiamide, and thiourea. This material is a polymeric semiconductor consisting predominantly of carbon and nitrogen atoms forming planar tri-*s*-triazine (or heptazine) π -conjugated layers. As a rule, this material has rather low photocatalytic activity due to small specific surface, low concentration of active sites, and low mobility of photogenerated charges, leading to rapid charge recombination. Hence, various approaches have been developed for improving the physicochemical characteristics of g-C₃N₄ by modification with organic and inorganic compounds, exfoliation, creation of spatially-organized structures and hybrid (composite) materials derived from g-C₃N₄ and other compounds [2, 3, 9, 14, 15, 17, 19, 22, 32, 43-48]. Furthermore, the structure of GCN consisting of virtually separate polyheptazine layers of atomic thickness provides for an unprecedented broad range of possibilities for structural variation by the introduction of separate chains of other heterocycles, replacement of nitrogen atoms by other heteroatoms such as phosphorus, sulfur, and boron, and creation of nitrogen and carbon vacancies [12-17, 19, 47, 49]. In addition, altering the nature of the hydrogen bonds between individual polyheptazine chains can affect the topology of the sheets and form various spatial structures, in particular, nano- and microrods, nano- and microtubes of g-C₃N₄. Finally, chemical and/or mechanical action on layered g-C₃N₄ can lead to its exfoliation into ultrathin plates (with thickness of several sheets) and separate monolayers or, on the other hand, dispersion of the bulk material to give a nanosized state [6, 10, 11-17, 19, 25, 26, 30, 31, 47, 48, 50, 51]. The abovementioned factors illustrate the powerful arsenal of means for the design and control of the properties of graphitic carbon nitride, which are virtually unobtainable for typical inorganic semiconductor photocatalysts, in particular, for carrying out selective photocatalytic transformations.

The range of possibilities for altering the properties of g-C₃N₄ permits its fine tuning for each specific chemical transformation, creating energy conditions, surface acid-base balance, porosity, and spatial organization required for the reaction through a specific pathway. This property of g-C₃N₄ has been rather well elucidated for thermal catalytic transformations using this material [5, 6, 10, 14, 17]. On the other hand, the impressive potential of GCN in photocatalytic transformations, in particular, in selective organic reactions, has not yet been fully revealed.

In this review, we have attempted to summarize and analyze the current state of knowledge concerning photocatalytic systems derived from g-C₃N₄ for the selective oxidation of various organic compounds. Selective photocatalytic oxidative reactions are clearly the most typical and well-studied for g-C₃N₄ and give a good illustration of the major factors determining the efficiency and selectivity of this semiconductor as a photocatalyst of organic reactions.

Oxidative activation of C–H bonds

Activation of the C(sp³)–H bond. One of the most difficult problems in the organic synthesis of valuable oxygen-containing products is achieving the selective oxidation of saturated hydrocarbons since the C–H bonds in such compounds are quite inert. Yuan et al. [52]

studied the photochemical oxidation of methane when it is present in relatively low concentration (1000 ppm) in systems derived from graphitic carbon nitride. Only the complete oxidation of methane to CO and CO₂ takes place upon the irradiation of a mixture of CH₄ and air using light from a xenon lamp in the presence of bulk g-C₃N₄ synthesized by the pyrolysis of melamine. On the other hand, methanol is formed with selectivity $S = 52\%$ at a low rate (4.38 $\mu\text{moles/h}\cdot\text{g}$) when using a composite photocatalyst g-C₃N₄/Cs_{0.33}WO₃ obtained by treating tungsten bronze Cs_{0.33}WO₃ with an aqueous ethanolic dispersion of GCN. The active oxidizing agent is the O₂⁻ anion-radical formed when oxygen accepts an electron photogenerated in GCN, while the second component, Cs_{0.33}WO₃, inhibits the peroxide pathway leading to deep oxidation products.

Organic compounds containing electron-withdrawing groups more readily undergo C–H bond activation. Thus, Ilkaeva et al. [53] found that g-C₃N₄ participates in the aerobic oxidation of the methyl group in 2-(4-methylphenoxy)ethanol to give 4-(2-hydroxyethoxy)benzaldehyde upon the action of near UV light. The greatest activity and selectivity were demonstrated by carbon nitride samples obtained by the pyrolysis of melamine subjected to thermal exfoliation with subsequent hydrogen peroxide treatment: at high conversion ($X \approx 70\%$), the selectivity for the desired product is about 80%. These authors attributed the higher activity of the samples treated with H₂O₂ to better separation of the charges photogenerated in these materials. Studies using spin traps indicated that the active oxidizing species is the O₂⁻ anion-radical formed when an oxygen molecule accepts a photogenerated electron. The position of the methyl group relative to the oxyethanol fragment in the substrate molecule was found to have a significant effect on the extent of its conversion and selectivity relative to the oxidation product. Thus, in the photooxidation of 3-(2-methylphenoxy)ethanol to give 3-(2-hydroxyethoxy)benzaldehyde using the most active g-C₃N₄ samples, the conversion and selectivity do not exceed 42-46% and 38-39%, respectively. The photocatalytic conversion of (4-methylphenoxy)acetic acid proceeds with even less selectivity relative to the CH₃ group. Thus such modification of g-C₃N₄ is not optimal for the selective oxidation of this substrate.

Mesoporous carbon nitride (mpg-C₃N₄) passivated by melamine in order to eliminate various structural defects was used as a photocatalyst for the aerobic oxidation of 1,4-dihydro-2,6-dimethylpyridine-3,5-dicarboxylate upon the action of visible light, which permitted aromatization of pyridine ring in this compound [54]. Oxidation of this substrate in an inert atmosphere proceeded with the participation of photogenerated holes and the concurrent generation of hydrogen due to the reduction of liberated protons by photogenerated electrons.

High efficiency in the oxidative activation of the C(sp³)–H bond in a series of compounds was achieved in a binary photocatalytic system containing N-hydroxyphthalimide in addition to g-C₃N₄ [55]. The action of visible light on this system leads to the selective oxidation of cholesteryl acetate, cyclohexane, cyclohexene, phenylethylene, toluene, ethylbenzene, α -pinene, as well as α - and β -isophorone in the presence of oxygen to give the corresponding carbonyl compounds. The mechanism of the photocatalytic reaction presumably involves several steps: capture of a photogenerated electron from the conductance band of GCN by an oxygen molecule to give an O₂⁻ anion-radical, the reduction of this species by N-hydroxyphthalimide to give HOO⁻ and a nitroxyl radical >N–O[•], which abstracts a hydrogen atom from the substrate molecule to give the corresponding free radicals, leading to further transformations in the oxygen atmosphere to final oxygenated products.

Esterification could be carried out in high yields ($X = 91\text{--}96\%$) due to the oxidative activation of the C(sp³)–H bond in aromatic alcohols by the action of visible light in methanolic

solutions in the presence of air. This process involves g-C₃N₄ synthesized by the thermal polycondensation of urea with palladium nanoparticles immobilized on its surface [56]. The presence of electron-withdrawing (NO₂) and electron-donor substituents (CH₃, CH₃O, and OH) in the benzene ring did not have a significant effect on the reactivity of the substrates and yield of the final products, while furfuryl alcohol and 2-thiophenemethanol were converted to the corresponding methyl esters without the formation of any side-products.

Oxidative C–H bond activation in a series of hydrocarbons was carried out using bulk g-C₃N₄ with carbon nanoparticles immobilized on its surface [57]. Visible light irradiation of an aqueous suspension of this photocatalyst in an oxygen atmosphere at 30°C gave oxidized products with high selectivity: 77% benzaldehyde from toluene, 83.3% 4-anisylaldehyde from 4-methylanisol, 86.2% 4-fluorobenzaldehyde from 4-fluorotoluene, 76.9% acetophenone from phenylethane, and 87.4% 1-tetralone from 1,2,3,4-tetrahydronaphthalene.

The use of hydrogen peroxide as the oxidizing agent in a photocatalyst obtained by the immobilization of vanadyl acetylacetonate on carbon nitride (VO/g-C₃N₄) permitted C–H bond activation in ethylbenzene and a series of methylarenes containing various substituents (NO₂, Br, Cl, F, CH₃O, and CH₃) in the aromatic ring [58]. The corresponding aldehydes and ketones were obtained in high yield upon irradiation of the reaction mixtures with visible light. Aromatic hydrocarbons containing a methylene fragment in cyclic structures were found more reactive than the corresponding open-chain substrates [58]. The proposed reaction mechanism entailed the generation of radical species formed on the vanadium site of an oxirane ring, which reacts with an alkyl radical and then undergoes rearrangement to give the final product and regeneration of the photocatalyst [58]. The role of GCN as a component of the VO/g-C₃N₄ photocatalyst was not completely elucidated by Verma et al. [58], who only noted that it is a better support than unmodified graphene oxide, nitrogen-doped graphene oxide, and titanium dioxide.

The composite photocatalyst FeVO₄/g-C₃N₄ obtained by heat treatment of a mixture of ferric vanadate and GCN synthesized by the pyrolysis of melamine was also used to activate the aliphatic C–H bonds in toluene, ethylbenzene, *para*-xylene, and diphenylmethane [59]. In the case of the latter two compounds, only the products of the activation of this bond were obtained in rather high yield: 34.4% 4-methylbenzaldehyde and 65.6% benzophenone, respectively.

Fig. 1. *a*) Mechanism for the oxidation of β-isophorone on carbon nitride, *b*) mechanism for the formation of dibenzyl disulfides with the participation of potassium polyheptazinimide (K-PHI) and elemental sulfur. Reprinted with the permission of Zhang [63] (*a*) and Savateev [64] (*b*). Copyright (2013, 2014) The Royal Society of Chemistry.

nm = nm для = for

Visible light irradiation of an aqueous suspension containing cyclohexane and a nanocomposite photocatalyst, Au/g-C₃N₄, obtained by the photoreduction of gold ions on bulk GCN synthesized by the pyrolysis of urea gives cyclohexanone with ~11% conversion and 100% selectivity without additional oxidizing agents [60]. The use of a series of spin traps indicated that the oxidizing species is the OH radical formed upon the decomposition of H₂O₂, which is the product of the oxidation of water by holes photogenerated in g-C₃N₄.

Virtually the same efficiency ($X = 8.62\%$, $S \approx 99\%$) was achieved in the oxidation of cyclohexane to give cyclohexanone in an aqueous medium by the action of visible light at 60°C in the absence of oxidizing agents using a composite photocatalyst $\text{Ag}_3\text{PW}_{12}\text{O}_{40}/\text{g-C}_3\text{N}_4$ obtained upon the consecutive treatment of GCN by solutions of AgNO_3 and $\text{H}_3\text{PW}_{12}\text{O}_{40}$ [61].

Zhang et al. [62] also studied the selective oxidation of cyclohexane to give cyclohexanone ($S = 99.9\%$) by the action of near UV light (365 nm) in the presence of mpg- C_3N_4 subjected to additional heat treatment in a molten mixture of lithium and potassium chlorides. The conversion of cyclohexane over 48 h in the presence of air was 5.81%, while this conversion in an oxygen atmosphere was 12.1%. The use of spin traps showed that radicals O_2^- and HO^\bullet generated by means of photoexcited GCN also participate in this reaction.

Mesoporous g- C_3N_4 , which is the product of the thermal condensation of cyanamide in the presence of SiO_2 nanoparticles with their subsequent removal by treatment with an aqueous solution of NH_4HF_2 , was subjected to post-synthetic chemical modification by means of 1,3-dipolar cycloaddition of azomethine ylids. The modification took place through *in situ* thermal condensation of N-methylglycine and a series of aldehydes containing phenyl, pyridinium, N-butylpyridinium bromide, and ferrocene functional groups [63]. These materials were used for the selective aerobic oxidation of the allyl C–H bond in β -isophorone by the action of visible light to give *keto*-isophorone (KIP), which has found use in the synthesis of vitamins and carotenoids. Greatest efficiency was demonstrated for samples synthesized using aldehydes with N-butylpyridinium ($S = 92\%$) and ferrocene groups ($S = 84\%$). Side-products α -isophorone (α -IP) and 4-hydroxy-3,5,5-trimethyl-2-cyclohexen-1-one (HIP) were formed in small amounts. The proposed mechanism for the oxidation of β -isophorone (β -IP) on carbon nitride is presented in Fig. 1a.

Savateev et al. [64] activated the C–H bond in some substituted methylenes in the presence of elemental sulfur as the oxidizing agent using potassium polyheptazinimide (K-PHI) synthesized by the thermolysis of 5-aminotetrazole in an LiCl/KCl eutectic mixture. A series of dibenzyl disulfides was obtained in 41–67% yield upon irradiation of argon-saturated reaction mixtures with a light diode (461 nm) at 50°C for 24 h. The mechanism shown in Fig. 1b assumes participation of both charges photogenerated in K-PHI, namely, an electron for the activation of sulfur to give its anion-radical S_8^- and a hole, which activates the methylene to give its cation-radical. The reaction of these radical species then leads to the formation of an unstable intermediate, which converts into the desired product, dibenzyl disulfide, with the release of hydrogen sulfide.

TABLE 1. Photocatalytic Properties of Materials Derived from g- C_3N_4 in the Hydroxylation of Benzene by Hydrogen Peroxide to Give Phenol

Photocatalyst, mg	S_{sp} , m^2/g	B, ml	H_2O_2 , ml	Medium (ml)	$T, ^\circ\text{C}$	t , h	λ_{irr} , nm	Y , %	Ref.
-------------------	---	-------	-----------------------------	-------------	---------------------	---------	-----------------------------	---------	------

B.P. = W.S.

Note: B) benzene, t) reaction time, Y) yield, SBA-15) mesoporous silica, TS-1) titanosilicate, W.S.) without solvent, ^ammoles, ^b30% H_2O_2 , irradiation source, ^c500-W xenon lamp, ^d300-W xenon lamp, ^e25% H_2O_2 , ^f100-W Hg lamp, ^g20-W light diode,

Activation of C(sp²)-H bonds. The activation of the C(sp²)-H bond in aromatic hydrocarbons, for example, in the direct oxidation of benzene to give phenol under mild conditions using readily available oxidizing agents has attracted attention as an alternative to the well-known three-step reaction for the preparation of this valuable product from cumene. In particular, studies have been carried out on the possibility of a photocatalytic synthesis of phenol using photoactive materials derived from graphitic carbon nitride. As in other reactions, bulk GCN displays extremely low activity in the photocatalytic oxidation of benzene. Modified samples of carbon nitride or its derived composites have been used to enhance the efficiency of this material [59, 65-70]. Table 1 gives indices for the photocatalytic hydroxylation of benzene to give phenol using samples with an optimized composition. In comparison with bulk g-C₃N₄ obtained by the pyrolysis of dicyandiamide [66, 67], the phenol yield was enhanced using samples modified with transition metal ions, which form the activity series Fe > Cu > Mn > Ni > Co [66] and Fe > Ni > Zn > Co [67]. Greater activity was also observed upon the deposition of metal-modified g-C₃N₄ onto mesoporous supports, namely, SBA-15 silica [65-67] and titanosilicate TS-1 [67], which is likely related to enhanced specific surface.

Much higher efficiency was achieved using a bimetallic nanocomposite Au-Pd/g-C₃N₄ synthesized by the pyrolysis of a mixture of melamine treated with copolymer Pluronic P123 as well as palladium salt solutions and gold nanoparticles stabilized by polyvinylpyrrolidone prepared by laser ablation [68]. We should note that a rather high yield was also found when the reaction was carried out without any solvent (Table 1).

The hydroxylation of benzene by hydrogen peroxide upon the action of visible light was studied using a series of photocatalysts obtained by the treatment of bulk g-C₃N₄ prepared by the pyrolysis of melamine using solutions of the salts of two different metals (Fe and Pd, Fe and Au, Cu and Pd, Au and Pd, Cu and Au) with subsequent reduction by sodium borohydride [69]. All these composites displayed low activity with the exception of Cu-Au/g-C₃N₄ with the smallest band gap width ($E_g = 2.27$ eV), which is a better absorber of visible light. The conversion of benzene with virtually quantitative yield was achieved with the Cu-Au/g-C₃N₄ photocatalyst upon irradiation for 0.5 h at room temperature (Table 1).

Samanta and Srivastava [59] also studied the hydrogen peroxide hydroxylation of benzene, phenol, hydroquinone, naphthalene, and anthracene using the abovementioned photocatalyst FeVO₄/g-C₃N₄. Rather high yields of phenol (Table 1) were also achieved in the photocatalytic hydroxylation of benzene using mpg-C₃N₄ modified with ferrocenecarboxylic acid (Fc-CO₂H) [70]. This acid acts a cocatalyst in the conversion of benzene into phenol by accepting electrons from the GCN conductance band and transferring them to H₂O₂ molecules.

Schemes for the mechanism of the hydroxylation of benzene proposed by various authors [59-70] entail the dissociation of H₂O₂ into OH⁻ and HO[•] upon the reaction of photogenerated electrons with hydrogen peroxide with subsequent addition of the hydroxyl radical to a benzene molecule and dissociation of the resultant intermediate into protons and phenol.

Oxidative activation of the C=C bond in alkenes

The selective epoxidation of cyclooctene without additional oxidation agents was carried out with the abovementioned composite Ag₃PW₁₂O₄₀/g-C₃N₄ by the action of visible light in an aqueous medium at 60°C. The conversion relative to cyclooctene was 41.26% and the selectivity relative to epoxycyclooctane was up to 77.2% [61]. Ding et al. [66] showed the possibility of

oxidation of styrene to epoxystyrene by oxygen in a dimethylformamide solution by the action of light with $\lambda > 420$ nm using bulk g-C₃N₄ obtained by the pyrolysis of dicyandiamide ($S = 53.0\%$) as well as GCN samples doped with cobalt ($S = 58.5\%$) and iron ($S = 66.6\%$).

Activation of the C–OH bond

The selective oxidation of alcohols to the corresponding aldehydes or ketones is one of the most important reactions in organic synthesis. In comparison with traditional chemical methods, which are usually carried out at high temperature and pressure using dangerous and harmful compounds such as organic peroxides and metal oxides, processes using light energy including photocatalytic reactions hold promise for the activation of the O–H bond.

Low reactivity is found for saturated alcohols, similar to saturated hydrocarbons, in photocatalytic reactions and this apparently accounts for the sparse data in the literature on such reactions involving g-C₃N₄. Thus, the use of bulk GCN with surface-immobilized carbon nanoparticles gives oxidative activation of the O–H bond in cyclohexanol, 2-cyclohexen-1-ol, 2-methyl-2-cyclohexen-1-ol, 3-methyl-2-cyclohexen-1-ol, 3,5,5-trimethyl-2-cyclohexen-1-ol, 1,2,3,4-tetrahydronaphthol, and carverol to give the corresponding ketones [57]. The most efficient oxidation was found for allylic alcohols, while the oxidation of alcohols such as cyclohexanol proceeds much more slowly.

3-Pentanol ($t = 10$ h, $X = 55\%$, $S = 100\%$) [71] and 2-heptanol ($t = 1.5$ h, $X = 3\%$, $S = 100\%$) [72] are oxidized by molecular oxygen to ketones in the presence of mpg-C₃N₄ samples by the action of light at 100°C and pH 0. Cinnamyl alcohol ($t = 20$ h, $X = 55\%$, $S = 61\%$) and cyclohexanol ($t = 20$ h, $X = 37\%$, $S = 78\%$) are oxidized to the corresponding carbonyl compounds using a composite photocatalyst derived from bulk GCN with surface-supported platinum nanoparticles upon irradiation with visible light in an inert atmosphere. Electrons obtained upon the oxidation of alcohols are consumed in the reduction of water to give molecular hydrogen [73]. A photocatalytic system derived from mpg-C₃N₄ and N-hydroxyphthalimide was used for the oxidation of cyclohexanol to cyclohexanone ($t = 17$ h, $X = 100\%$, $S = 97\%$) by oxygen in acetonitrile solutions upon the action of visible light with $\lambda > 420$ nm [74].

TABLE 2. Photocatalytic Properties of Bulk, Modified and Alloyed g-C₃N₄ in the Oxidation of Benzyl Alcohol (BA) to Give Benzaldehyde

Photocatalyst, mg S_{sp} , m²/g E_g , eV BA, mM/liter P_{O_2} , MPa Medium, ml T , °C t , h λ_{irr} , nm X , % S , % Ref.

ГНУ = GCN ЦА = CA ДЦДА = DCDA ГНУ-М = GCN-M ГНУ-У = GCN-U CyA = CUA
g-ГНУ-М(Кр) = g-GCN-M(Cr) БФ = WF ТФМБ = TFMB Толуол = Toluene TP = TE

Notes: X) conversion, S) selectivity, CUA) cyanuric acid, ATCN) 3-aminothiophene-2-carbonitrile, TFMB) trifluoromethylbenzene, WF) irradiation without filter, M) melamine, TE = thermal exfoliation, ^aair, irradiation source, ^b300-W Xe lamp, ^d100-W halogen lamp, ^e200-W white light lamp, ^glight diode, ^cQuantum yield, ^fmicroliters, ^hsample treated with H₂SO₄, ⁱsample exfoliated at 500°C, ^jsample treated in melt of KCl + LiCl, ^ksample treated with HNO₃.

The selective photocatalytic oxidation of benzyl and other aromatic alcohols using GCN materials was studied much more extensively.

Samples of bulk GCN synthesized by the thermal polycondensation of cyanamide [71, 72], dicyandiamide [75, 76], melamine [77-79], urea, and thiourea [79] display low activity in the oxidation of benzyl alcohol and other aromatic alcohols. Table 2 shows that the irradiation of solutions of benzyl alcohol in various solvents with visible and UV light at room and elevated temperatures leads to the selective photocatalytic formation of benzaldehyde on samples of g-C₃N₄ synthesized from cyanamide, dicyandiamide, melamine, and urea in greater amounts than on a sample synthesized from thiourea. Benzaldehyde is obtained with >99% selectivity also in the absence of any oxidizing agent with the concurrent generation of molecular hydrogen [76]. In comparison with the starting materials prepared from melamine [79] or dicyandiamide [76], samples after thermal exfoliation displayed much higher activity; the conversion and selectivity relative to benzaldehyde were much higher upon the action of both visible and UV light (Table 2). Similar behavior but with even higher conversion (42%) and selectivity relative to aldehyde formation (84%) were found in the oxidation of 4-methoxybenzyl alcohol [79]. In comparison with benzyl alcohol, piperonyl alcohol also proved more reactive in photocatalytic oxidation with these samples [79] but the selectivity in all cases was lower than in the oxidation of benzyl and 4-methoxybenzyl alcohols, probably due to the instability of the five-membered ring containing a methylenedioxy group in the oxidizing medium, leading to partial extensive oxidation of this substrate. As a rule, the conversion using all the samples upon irradiation with visible light is lower than upon the action of UV light, which can be attributed to the greater light absorption in the UV spectral range and more efficient generation of the primary radical species, namely, superoxide ion-radicals responsible for oxidation of the alcohol.

The extent of conversion of the substrates studied was higher when using modified GCN prepared by the pyrolysis of a mixture of melamine and cyanuric acid (g-C₃N₄-M-CUA) due to enhanced specific surface but the selectivity relative to benzaldehyde (Table 2) and piperonal was lower [79].

In order to increase the activity of bulk g-C₃N₄ prepared by the pyrolysis of dicyandiamide, this material was treated with hot solutions of sulfuric, nitric, hydrochloric, phosphoric, formic, acetic, benzenesulfonic, and perchloric acids. The resultant materials were used as photocatalysts for the aerobic oxidation of benzyl alcohol upon visible light irradiation [75]. The greatest efficiency ($t = 10$ h, $X = 23.4\%$, $S > 99\%$) and stability in a cyclic process were found for samples modified by sulfuric acid due to increased band gap width and specific surface area, decreased particle size, improved adsorption properties of the surface, and enhanced separation of the photogenerated charges.

For the same purpose, Lima et al. [76] subjected g-C₃N₄ obtained by the thermal condensation of dicyandiamide to several additional types of treatment, including heating at 400, 450, and 500°C, mechanical treatment in a ball mill, and chemical treatment in concentrated H₂SO₄, HCl, and HNO₃. The resultant materials were tested in the photocatalytic oxidation of benzyl alcohol to give benzaldehyde in an aqueous argon-saturated solution. Under these conditions, the reaction proceeds through the direct oxidation of the alcohol by photogenerated holes, while the liberated protons are reduced by photogenerated electrons to give molecular hydrogen. The highest activity ($X = 66\%$, $S = 90\%$) upon irradiation by a light diode source at 392 nm was found for the material obtained by additional treatment at 500°C due to significant

enhancement of the specific surface from 4 to 87 m²/g and greater hydrophobicity, which facilitates a tighter interaction of the substrate molecules with the photocatalyst surface.

A considerably higher rate of photocatalytic aerobic oxidation of benzyl and other aromatic alcohols containing various substituents in the benzene ring such as NO₂, Cl, CH₃O, and CH₃ was also achieved using GCN prepared by the thermal condensation of melamine previously treated with nitric acid [78]. In comparison with the starting material, the sample prepared by this method contained nitrogen atom vacancies in the polyheptazine network of g-C₃N₄ bound by three adjacent heptazine rings, had enhanced surface area, greater optical absorption, and concurrently acted as a trap for electrons or holes. This enhanced the efficiency of the separation of the photogenerated charges in the material, enhancing its photocatalytic activity.

Benzyl and methoxybenzyl alcohols were oxidized to the corresponding aldehydes in aqueous solution by the action of sunlight in a pilot plant using thermally-exfoliated carbon nitride prepared by the pyrolysis of melamine and also after additional treatment of the resultant material with hydrogen peroxide [81, 82]. The alcohols were oxidized at a greater rate but with lower selectivity in the presence of thermally-exfoliated g-C₃N₄ with enhanced specific surface area (129 and 59 m²/g).

Fig. 2. *a, c*) Mechanism for the photocatalytic oxidation of benzyl alcohol in the presence of potassium polyheptazinimide (K-PHI) and sulfur as the electron acceptor (*a*) and mesoporous GCN and N-hydroxyphthalimide (*c*); *b*) mechanism for the oxidation of alcohols using carbon nitride. Reprinted with permission [82] (*a*), [72] (*b*), and [74] (*c*). Copyright (2015, 2017) Elsevier (*a, c*) and (2010) American Chemical Society (*b*).

Отрыв водорода = Hydrogen abstraction Отрыв H⁺ = Abstraction of H⁺ нм = nm

Bellardita et al. [79] studied the oxidation of benzyl alcohol, 4-methylbenzyl alcohol, and piperonyl alcohol in aqueous media upon irradiation with UV and visible light using GCN samples prepared by the pyrolysis of phosphorus-doped melamine, urea, and thiourea. The samples doped with phosphorus proved less active than the initial materials but they displayed greater selectivity relative to the formation of benzaldehyde and methoxybenzaldehyde (82-100%) upon the action of UV light.

Zhou et al. [77] also found that g-C₃N₄ prepared by the pyrolysis of urea and subjected to additional heat treatment in a molten KCl/LiCl was an efficient photocatalyst for the selective aerobic oxidation of a series of substituted aromatic alcohols. In the oxidation of benzyl alcohol, the conversion was 52.2% and the selectivity relative to benzaldehyde formation was 92.6% (Table 2). The good photocatalytic properties of the resultant material were attributed to efficient separation of the photogenerated charges and better adsorption indices relative to the alcohol and oxygen as well as desorption indices relative to the aldehyde reaction product. The improvement in the functional properties of this material can also be related to the presence of potassium, which penetrates the g-C₃N₄ structure during the heat treatment in the molten salt mixture.

Potassium polyheptazinimide obtained by the thermolysis of a mixture of 5-aminotetrazole in the LiCl/KCl eutectic after its mechanochemical treatment proved a highly-efficient photocatalyst for the oxidation of benzyl alcohol to give benzaldehyde (*X* > 99%,

$S > 98\%$) by the action of visible light using elemental sulfur as the acceptor of photogenerated electrons [83]. According to Savateev et al. [83], sulfur has a number of advantages over other oxidizing agents although hydrogen sulfide, a toxic reduction product, is formed in this case (see the scheme in Fig. 2a).

Chen et al. [80] studied the photocatalytic oxidation of various alcohols by oxygen in the presence of mpg-C₃N₄ [71,72] as well as modified mesoporous g-C₃N₄ prepared by the thermal copolymerization of diacetamide and 3-amino-2-carbonitrile in the presence of Ludox-HSO₄ with its subsequent removal (Table 2). These alcohols included 1-phenylethanol, benzyl alcohol, 4-methoxybenzyl alcohols, and a series of other aromatic alcohols containing electron-withdrawing and electron-donor substituents (NO₂, Cl, F, and CH₃) in the *para* position and their oxidation gave the corresponding aldehydes with 90-97% selectivity. High chemoselectivity was found relative to oxidation of the benzylic alcohol group; a second –OH group when present in the aliphatic substituent was not oxidized [72]. Apparently, this behavior is related to the greater stability of the intermediate aromatic alkoxy radical relative to other possible intermediates. Spin traps were used to establish that the oxidizing agent is the superoxide anion-radical O₂^{•−}, which is formed upon the reduction of oxygen by the electrons photogenerated in the conductance band of GCN. The proposed mechanism of this photocatalytic oxidation of alcohols is shown in Fig. 2b.

TABLE 3. Photocatalytic Properties of Composites Derived from g-C₃N₄ in the Oxidation of Benzyl Alcohol (BA) to Give Benzaldehyde

Photocatalyst, mg	S_{sp} , m ² /g	E_g , eV	BA, mm	P _{O₂} , MPa	Medium, ml	T , °C	t , h	λ_{irr} , nm	X , %	S , %	Ref.
-------------------	------------------------------	------------	--------	----------------------------------	------------	----------	---------	----------------------	---------	---------	------

$T_K = RT$

Notes: RT) room temperature, ^ammoles H₂O₂; irradiation source, ^b40-W household lamp, ^cyield, ^dmicroliters, ^e200-W white light lamp, ^flight diode, ^g300-W Xe lamp, ^hair, ⁱ125-W Hg lamp, ^j250-W Hg lamp, ^k500-W Xe lamp,

Zheng et al. [84] prepared a series of 1,2-diketones in high yield (49-73%) from α -hydroxyketones with electron-donor and electron-withdrawing ring substituents (CH₃, C₂H₅, CH₃O, Cl, Br) and carried out their aerobic oxidation at 100°C by the action of visible light using mpg-C₃N₄ as the photocatalyst. Zhang et al. [74] used a photocatalytic system derived from mesoporous g-C₃N₄ in combination with an organic cocatalyst (N-hydroxyphthalimide) for the selective aerobic oxidation of benzyl, 4-methylbenzyl, 4-methoxybenzyl, and 4-nitrobenzyl alcohols as well as benzhydrol and 4,4'-dichlorobenzhydrol at room temperature in acetonitrile solution by the action of light with $\lambda > 420$ nm. In the case of benzyl alcohol and up to 5% organic cocatalyst, the major product was cyclohexanone, while benzoic acid was the major product when the content of organic cocatalyst was higher. A spin trap study suggested a probable mechanism (Fig. 2c) entailing, as in the abovementioned work of Zhang et al. [55], the acceptance of electrons photogenerated in carbon nitride by O₂ molecules, reduction of the resultant O₂^{•−} anion-radicals by N-hydroxyphthalimide to give HOO[−] and a nitroxyl radical

$>\text{N}-\text{O}^\bullet$, which induces further radical transformations of the alcohol molecules to give the oxidized products.

In addition to these pure and doped GCN samples, various composite materials derived from g-C₃N₄ were studied as photocatalysts for the oxidation of benzyl alcohol and its derivatives. Thus, the O–H bond was activated in benzyl (Table 3) and other aromatic alcohols containing electron-donor and electron-withdrawing groups (NO₂, CH₃O, and CH₃) as well as in 2-thiophenemethanol, furfuryl alcohol, cyclohexanol, 1,2-cyclohexanediol, and 2-hydroxy-1,2-diphenylethanol using the photocatalyst VO_x/g-C₃N₄ prepared by immobilization of vanadium acetylacetonate on carbon nitride using H₂O₂ as the oxidizing agent [85]. The corresponding aldehydes and ketones, including diketones from the two latter substrates, were obtained in high yield (85-98%) upon visible light irradiation of the reaction mixtures.

Fig. 3. *a*) Conversion (*X*) of benzyl alcohol, selectivity relative to benzaldehyde formation (*S*), and benzaldehyde yield (*Y*) in the photocatalytic oxidation of benzyl alcohol in the presence of GCN heterostructures with metal nanoparticles, *b*) mechanism for the oxidation of alcohols using MgO/g-C₃N₄, *c*) products of the oxidation and oxidative methylation of benzyl alcohol using photocatalyst (PC) BiVO₄/g-C₃N₄, *d*) energy scheme for photoinduced electron transfer in the linked reduction of nitrobenzene and oxidation of alcohols using CdS/g-C₃N₄. Reprinted with permission [86] (*a*), [87] (*b*), [88] (*c*), and [89] (*d*). Copyright (2014, 2016) Elsevier (*a*, *d*), (2018) The Royal Society of Chemistry (*b*), (2017) American Chemical Society (*c*).

ФК = PC Потенциал, эВ отн. НБЕ = Potential, eV rel. NHE

Zhang et al. [57] oxidized 1-phenylethanol as well as benzyl, 4-methoxybenzyl, and 4-fluorobenzyl alcohols to give the corresponding carbonyl compounds using oxygen under mild conditions in the presence of bulk GCN with surface-immobilized carbon nanoparticles by the action of visible light. The photocatalytic conversion of benzyl alcohol into benzaldehyde was carried out with the concurrent generation of molecular hydrogen (Table 3) using a composite photocatalyst prepared by the deposition of nanoparticles of Au, Ru, Pd, Pt, Ir, Ag, and Rh onto the surface of bulk GCN in acidic aqueous media without oxidizing agents [86]. These composite photocatalysts were more active than the initial g-C₃N₄ sample due to efficient separation of the photogenerated charges but differ somewhat in regard to the conversion of benzyl alcohol and selectivity relative to the formation of the desired product, benzaldehyde. Although the greatest conversion was achieved using the Au/g-C₃N₄ composite, the Ru/g-C₃N₄ composite, containing the smallest metal particles (5 nm), featuring the narrowest band gap width (2.66 eV), and displaying the best selectivity, was considered the optimal photocatalyst. Use of this photocatalyst gave 73% alcohol conversion and 72% selectivity relative to benzaldehyde formation at pH 2.0 after 4 h irradiation with a light diode source (390 nm) (Fig. 3*a*). We should note that the formation of benzoic acid was detected during this reaction as well as the possibility of complete oxidation of the substrate with yields of 17 and 10% using Au/g-C₃N₄ and Rh/g-C₃N₄, respectively.

The same process of concurrent photocatalytic generation of hydrogen from water and the conversion of benzyl, 4-methoxybenzyl, 4-methylbenzyl, and 4-chlorobenzyl alcohols to the corresponding aldehydes was achieved using a composite photocatalyst derived from bulk GCN

containing surface-anchored platinum nanoparticles [73]. The selectivity in the oxidation of substituted benzyl alcohols was low (51-67%) due to more extensive oxidation of the resultant aldehydes by photogenerated holes of the valence band of g-C₃N₄ with a rather high oxidation potential ($E_{VB} = 1.4$ V). In the case of 4-methoxybenzyl alcohol, the selectivity relative to aldehyde formation can be significantly enhanced to >99% by using the ruthenium complex [Ru(tpa)(H₂O)₂](PF₆) (tpa = tris(2-pyridylmethyl)amine), which has a lower oxidation potential and can act as mediator of the photogenerated holes.

Kasap et al. [90] found that a hybrid photocatalytic system derived from GCN functionalized with cyanamide and a molecular hydrogen generation catalyst, namely, nickel(II) bis(diphosphine), proved to be much more efficient in the conversion of 4-methylbenzyl alcohol to give 4-methylbenzaldehyde with the concurrent generation of hydrogen in an aqueous solution at pH 4.5. The alcohol conversion under optimal conditions was $83.0 \pm 8.3\%$ with 100% selectivity relative to aldehyde formation.

A study of this system showed that the GCN used is capable of the capture and prolonged storage of photogenerated electrons due to efficient acceptance of photogenerated holes by substrate molecules as indicated by the appearance of a characteristic blue color during the irradiation corresponding to an absorption band with maximum at $\lambda = 650$ nm. This behavior may be ascribed to forming "hot" carriers upon photoexcitation of the polymeric photocatalyst due to more rapid dissociation of the excitons on the boundary between ordered and disordered regions [91]. There is an approximately seven-fold increase in the concentration of electrons relative to the starting sample of g-C₃N₄ due to the injection of electrons into the ordered chains and blockage of the holes in the disordered sites of the resultant polycrystalline carbon nitride. As a consequence, the polycrystalline sample demonstrated higher activity upon the action of visible light with the participation of photogenerated electrons in processes such as the formation of superoxide radicals and the selective oxidation of benzyl alcohol and its substituted derivatives containing electron-donor and electron-withdrawing groups (NO₂, F, Cl, Br, and CH₃) in the ring when using oxygen as the oxidizing agent [91].

Ramacharyulu [87] and Cerdan [92] also used composites derived from GCN and some metal oxides as photocatalysts for the selective oxidation of benzyl alcohols. Thus, the oxidation of benzyl alcohol by atmospheric oxygen in acetonitrile solutions by the action of near UV light ($\lambda = 365$ nm) was carried out using composite photocatalysts ZnO/g-C₃N₄ and Fe₂O₃/g-C₃N₄ obtained by a mechanochemical method [92]. Fe₂O₃/g-C₃N₄ proved the more active catalyst: after 4 h irradiation, the alcohol conversion was 20% and the selectivity relative to benzaldehyde formation was 70% (Table 3). The aerobic oxidation of benzyl, 4-chlorobenzyl, and 4-methylbenzyl alcohols also proceeded using the MgO/g-C₃N₄ composite obtained by the thermal polycondensation of melamine in the presence of magnesium oxide [87]. These alcohols in aqueous solution were converted to the corresponding aldehydes with selectivity 92.9, 90, and 90%, respectively with yields 72.4, 67, and 60.5%, respectively, at an optimal ratio of the components in the composite and after irradiation for 24 h with a light diode source ($\lambda = 550$ nm). The results of a spin trap study suggested a mechanism entailing initiation of the process with the participation of both photogenerated electrons and holes.

Samanta et al. [88] proposed a similar mechanism for the oxidation of benzyl alcohol by oxygen and hydrogen peroxide in acetonitrile solutions by the action of visible light, in which the composite BiVO₄/g-C₃N₄ prepared by heat treatment of a mixture of bismuth vanadate and GCN as the photocatalyst. The reaction products were benzaldehyde (BA) as well as benzyl benzoate (BB) formed upon the reaction of benzyl alcohol and benzoic acid, which is the product

of the oxidation of benzaldehyde. For a 1:1 mass ratio of the composite components, irradiation of the reaction mixture for 16 h in the presence of O₂ gave alcohol conversion and selectivity for the formation of benzaldehyde and benzyl benzoate as follows: $X = 81.3\%$, $S_{BA} = 77.3\%$, $S_{BB} = 22.7\%$. When H₂O₂ was used as the oxidizing agent, the values of $X = 57.8\%$, $S_{BA} = 65.5\%$, and $S_{BB} = 34.5\%$ were obtained. When the oxidation of benzyl alcohol in the presence of O₂ was carried out in methanolic solutions (Fig. 3c), dimethoxymethylbenzene (DMOB) and methyl benzoate (MB) were also obtained in addition to the abovementioned products ($X = 79.4\%$, $S_{BA} = 32.1\%$, $S_{BB} = 15.3\%$, $S_{DMOB} = 51.2\%$, and $S_{MB} = 1.4\%$). The higher activity of the BiVO₄/g-C₃N₄ composite than for the individual components is attributed to greater visible light absorption due to narrowing of the band gap as well as efficient separation of the photogenerated electron-hole pairs on the interface between BiVO₄ and GCN in the BiVO₄/g-C₃N₄ heterojunction.

Nanoporous GCN functionalized by propargyl alcohol with subsequent linking of an azido-containing bipyridyl cobalt complex to its surface was used for the direct photocatalytic synthesis of esters formed upon the oxidation of a series of benzyl alcohols in methanolic and ethanolic solutions [93]. Methyl and ethyl esters of benzoic acid containing various ring substituents (*p*-CH₃, *m*-CH₃, *m*-NH₂, *p*-Cl, *p*-NO₂, and *o*-NO₂) were obtained upon irradiation of the reaction mixtures with visible light at room temperature. Song et al. [94] studied the formation of esters of benzoic acid using bulk carbon nitride in the oxidation of benzaldehyde by hydrogen peroxide in acidified solutions of ethanol, 1-propanol, 2-propanol, 1-butanol, 1-pentanol, and 1-octanol by the action of light with $\lambda > 420$ nm. An increased rate was found when the composite photocatalyst SnO₂/g-C₃N₄ was used.

The ternary nanocomposite obtained by the immobilization of GO (graphene oxide) on protonated GCN with the subsequent synthesis of BiOCl *in situ* on the surface of g-C₃N₄/GO by means of a hydrothermal reaction and concurrent reduction of GO proved an active photocatalyst for the oxidation of benzyl alcohol to give benzaldehyde in acetonitrile solutions [95]. Irradiation of the reaction mixture with the artificial sunlight for 10 h gave 71.6% alcohol conversion and >99% selectivity relative to benzaldehyde formation (Table 3). Analysis of the energy diagram of the nanocomposite indicated that the photocatalytic process can be described in terms of a Z scheme assuming participation of the electrons and holes generated in bismuth oxychloride and carbon nitride connected by an electron transport layer consisting of reduced GO.

Reduced GO (RGO) was also used to obtain a composite with sandwich structure derived from the C₃N₃S₃ (triazine thiolate) polymer with conjugated π -bonds [96]. This composite was used to achieve 100% selectivity in the aerobic photocatalytic oxidation of benzyl, 4-nitrobenzyl, 4-fluorobenzyl, and 4-methylbenzyl alcohols in trifluoromethylbenzene solutions upon the action of visible light. The conversion of the substrates was approximately twice as great as in the presence of C₃N₃S₃ by itself. The alcohol conversion after 8 h irradiation formed the following series in decreasing order: CH₄ (54.4%) > H (51.5%) > NO₂ (34.1%) > F (25.4%). The greatest quantum yield (2.3%) was achieved in the oxidation of benzyl alcohol upon irradiation by light with $\lambda = 450$ nm. Xu et al. [96] proposed that the higher activity of the composite was mainly a function of its unique layered structure providing tight contact between the RGO and C₃N₃S₃ polymer components and facilitating transport of a photogenerated electron from C₃N₃S₃ to RGO; reduction of an O₂ molecule occurs on the RGO surface to give a superoxide ion-radical responsible for oxidation of the substrates.

Cross-linked photocatalytic selective oxidation of benzyl, 4-methoxybenzyl, 4-chlorobenzyl, 4-fluorobenzyl, and cinnamyl alcohols to the corresponding aldehydes and the

reduction of nitrobenzene to aniline was carried out with a composite photocatalyst CdS/g-C₃N₄ obtained by the hydrothermal synthesis of cadmium sulfide in the presence of bulk g-C₃N₄ [89]. The highest conversion and selectivity indices when the reaction was carried out in trifluoromethylbenzene solutions in an inert atmosphere at 60°C after 4 h irradiation were achieved for 4-methoxybenzene alcohol ($X=56\%$, $S=95\%$), while the lowest such indices were obtained for cinnamyl alcohol ($X=36\%$, $S=51\%$). The activity of the composite photocatalyst is much higher than for its individual components due to efficient separation of the photogenerated charges, which induce the oxidation-reduction transformations of the substrate molecules due to a favorable arrangement of the allowed bands of the heterostructure components (Fig. 5d).

Oxidative activation of the OH bond using various GCN photocatalysts [80, 81, 97-100] was also carried out in 5-hydroxymethyl-2-furfural (HMF), which is a cellulose treatment product, to give 2,5-furandicarboxaldehyde (2,5-diformylfuran (DFF)) and 2,5-furandicarboxylic acid, which have useful properties, especially in the production of biopolymers.

Using samples obtained by the pyrolysis of urea (U), thiourea (TU), and melamine (M) (Table 4), the greatest conversion of HMF ($X=44\%$) in its aerobic oxidation in aqueous solution after irradiation for 4 h with near UV light was achieved using GCN prepared from urea (g-C₃N₄-U), which can be attributed to the higher specific surface of this sample (28 m²/g) in comparison with GCN-TU and GCN-M obtained from thiourea (4 m²/g, $X=26\%$) and melamine (7 m²/g, $X=39\%$). The selectivity in the formation of DFF at 30% conversion is somewhat higher for the sample synthesized from melamine ($S=28\%$). After thermal exfoliation of this material at 540°C (g-C₃N₄-M-TE), its photocatalytic activity was much higher: the conversion of HMF was 69% with 43% selectivity. The relatively low selectivity relative to the desired product can be attributed to the formation of small amounts of 5-formyl-2-furoic acid and the complete oxidation of HMF, which proceeds, as proposed by Krivtsov et al. [97], by the action of UV light.

TABLE 4. Photocatalytic Oxidation of 5-Hydroxymethyl-2-furfural (HMF) in Systems Derived from g-C₃N₄ Under Optimal Conditions

Photocatalyst, mg	S_{sp} , m ² /g	HMF, mM	P _{O₂} , MPa	Medium, ml	T , °C	t , h	λ_{irr} , nm	X , %	S , %	Ref.
-------------------	------------------------------	---------	----------------------------------	------------	----------	---------	----------------------	---------	---------	------

TP = TE, TΦMB = TFMB БΦ = WF CC = SL

Notes: X) conversion, S) selectivity, TFMB) TFMB, SL) sunlight, WF) irradiation without filters, light source: ^a15-W fluorescent lamp, ^b300-W Xe lamp.

The higher selectivity in the aerobic oxidation of HMF to give DFF was shown by g-C₃N₄-M-TE prepared by the pyrolysis of melamine and subjected to additional heat treatment at 500°C in the presence of water, which led to an enhanced specific surface area and pore volume [98]. The highest yield of DFF (26.7%) in a mixture of polar solvents (acetonitrile + trifluoromethylbenzene) was achieved with 85.6% selectivity after 6 h irradiation using visible light with $\lambda > 400$ nm (Table 4). Data obtained using spin traps indicated that the

superoxide anion-radical O_2^- is the predominant active species in the photocatalytic oxidation of HMF [97, 98].

In the photocatalytic oxidation of HMF in aqueous solutions with irradiation by near UV light and natural sunlight, various authors [80, 81, 99] used thermally-exfoliated GCN (g-C₃N₄-TE) as well as materials subjected to additional treatment with hydrogen peroxide (g-C₃N₄-TE-H₂O₂) to give a stable adduct that does not release H₂O₂ into the reaction medium upon irradiation. Ilkaeva et al. [99] achieved 88% selectivity relative to DFF formation upon 20% conversion of HMF using optimal samples (Table 4) and natural sunlight. Ilkaeva et al. [99] proposed that the high selectivity using these materials could be a consequence of binding of H₂O₂ with GCN and the formation of a hydrogen bond network within the material. Furthermore, H₂O₂ molecules are capable of blocking NH₂ functional groups, which have an unfavorable effect on the selective oxidation of HMF to give DFF since water molecules coordinated with H₂O₂ molecules can undergo oxidation by photogenerated holes. The latter process gives OH radicals, which react with HMF leading to opening of the furan ring and the formation of aliphatic intermediates (Fig. 4a).

Approximately the same selectivity relative to DFF formation (87.2%) upon 27.4% conversion of HMF (Table 4) was achieved in the aerobic oxidation of HMF in a 3:2 mixture of acetonitrile and trifluoromethylbenzene by the action of visible light using a composite photocatalyst WO₃/g-C₃N₄ synthesized by the annealing of a mixture of ammonium tungstate and melamine [100]. The high photocatalytic activity was ascribed to the formation of heterostructures and a Z-scheme for the mechanism, facilitating separation of the photogenerated electrons and holes, which play an important role as active species inducing the transformation of HMF.

Fig. 4. *a*) Scheme for the mechanism of the photocatalytic oxidation of 5-hydroxymethylfurfural in the presence of GCN and adducts of GCN with H₂O₂, *b*) kinetic curves for the conversion of 5-hydroxymethylfurfural (HMF) and selectivity relative to the formation of 2,5-diformylfuran (DFF) and furandicarboxylic acid (FDCA) in a system derived from GCN and cobalt thioporphyrzine. Reprinted with permission [99] (*a*) and [101] (*b*). Copyright (2018) Elsevier (*a*) and (2017) American Chemical Society (*b*).

Раскрытие цикла = Ring opening

Алифатический интермедиат = Aliphatic intermediate

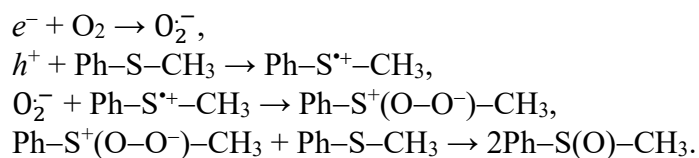
Конверсия = Conversion Время, ч = Time, h Селективность = Selectivity

The selective aerobic oxidation of 5-hydroxymethylfurfural to give 2,5-furandicarboxylic acid (FDCA) at room temperature upon the action of the artificial sunlight was carried out using GCN with surface-immobilized cobalt thioporphyrzine [101]. The high yield of FDCA (96.1%) was achieved by carrying out the oxidation in aqueous solution at pH \approx 9. The major product at pH 4 is 2,5-diformylfuran (Fig. 4*b*). The role of the cobalt complex was in the activation of O₂ molecules to give singlet oxygen 1O_2 , which is a mild oxidizing agent. Experimental evidence was obtained for a strong interaction between the components of the composite, which facilitates access to the reaction sites and excludes the generation of hydroxyl radicals that produce extensive oxidation of HMF to give CO₂ and H₂O.

Oxidation of organic sulfides

Sulfoxides occupy an important place among organosulfur compounds in organic chemistry due to their use in drug synthesis and agricultural chemistry. These compounds are obtained most frequently by the oxidation of sulfides using various chemical oxidizing agents and in catalytic reactions. In recent years, interest has arisen in photocatalytic systems for carrying out such reactions under mild conditions by the action of light, including processes using materials derived from GCN. Thus, the formation of sulfoxides using mpg-C₃N₄ as the photocatalyst was studied in the aerobic oxidation of methyl phenyl sulfide, its derivatives containing electron-donor (CH₃ and OCH₃) and electron-withdrawing substituents (Br, Cl, and NO₂) in the *para*-position of the benzene ring, as well as diphenyl sulfide and methyl furfuryl sulfide to give the corresponding sulfoxides (Fig. 7a) [102]. The efficiency of this reaction can be significantly enhanced in the presence of organic aldehydes. The highest conversion and selectivity in a study comparing the use of benzaldehyde, glyoxal, isobutyraldehyde, and formaldehyde were found for the reaction in the presence of isobutyraldehyde when this aldehyde was taken in a two-fold molar excess relative to mpg-C₃N₄ under optimal reaction conditions in 3 ml acetonitrile, 5 mg mpg-C₃N₄, 1 mmole substrate, and $\lambda_{\text{irr}} > 450 \text{ nm}$ at 25°C. The conversion of methyl phenyl sulfide after 4 h irradiation was 97% with 98% selectivity relative to the formation of methyl phenyl sulfoxide. The major reaction product in the case of a higher content of aldehyde or longer irradiation time becomes methyl phenyl sulfone, which is obtained upon the further oxidation of methyl phenyl sulfoxide.

The mechanism for the oxidation of this sulfide in the presence of only mpg-C₃N₄ assumes the participation of both photogenerated electrons and holes:



In the case of a binary system containing mpg-C₃N₄, the reaction mechanism based on the results obtained using spin traps (Fig. 5b) presumes participation of acyl radicals generated upon the abstraction of hydrogen atoms from two aldehyde molecules by the O₂⁻ anion-radicals (Fig. 5b, step 1). This process gives a peroxide radical or peracid as intermediates (Fig. 5b) capable of the facile oxidation of sulfides to yield the corresponding sulfoxides (Fig. 5b, step 3).

Fig. 5. a) Conversion of methyl furfuryl sulfide (1) and selectivity relative to the formation of methyl furfuryl sulfoxide (2) and methyl furfuryl sulfone (3) in the presence of mesoporous GCN and isobutyraldehyde, b) mechanism for the oxidation of sulfides in the presence of GCN and aldehyde, c) kinetic curves for the photocatalytic oxidation of benzothiophene (BT), dibenzothiophene (DBT), and 4,6-dimethyldibenzothiophene (4,6-DMDBT) using mesoporous GCN, d) conversion (1) and selectivity (2) of the oxidation of methyl *p*-methoxyphenyl sulfide in the presence of the GCN/CdS composite. Reprinted with permission [102] (a, b), [103] (c), and [105] (d). Copyright (2012) The Royal Society of Chemistry (a, b, d), (2016) Elsevier (c).

Время, ч = Time, h или = or Альдегид = Aldehyde
 Пероксирадикал или пероксикислота = Peroxy radical or peroxy acid
 Время, мин = Time, min

Mesoporous GCN, obtained by the pyrolysis of a mixture of cyanamide with silica nanoparticles as a template with subsequent removal of silica by treatment with 4 M aqueous NH_4HF_2 , was tested as a photocatalyst for the aerobic oxidation of benzothiophene, dibenzothiophene, and 4,6-dimethyldibenzothiophene as impurities in *n*-octane as a model motor fuel (Fig. 5c) [103]. These compounds upon irradiation of the reaction mixtures with visible light at room temperature were converted into the corresponding sulfones. The presumed oxidizing agent was the superoxide anion-radical photogenerated in carbon nitride upon acceptance of an electron by an oxygen molecule.

Sulfides such as $\text{CH}_3\text{--S--CH}_3$, $\text{C}_2\text{H}_5\text{--S--C}_2\text{H}_5$, Ph--S--Ph , Ph--S--CH_3 , *p*-BrPh-S- CH_3 , *p*-ClPh-S- CH_3 , *p*- $\text{CH}_3\text{OPh--S--CH}_3$, and *o*-BrPh-S- CH_3 were also aerobically oxidized almost quantitatively to the corresponding sulfoxides upon irradiation of their solutions in acetonitrile (0.5 mmole) with a 50-W xenon lamp for 8-16 h using g- C_3N_4 obtained by the pyrolysis of melamine and additional treatment with concentrated HNO_3 and H_2SO_4 [104]. The oxidizing agent in this system was singlet oxygen.

Methyl *p*-methoxyphenyl sulfide (Fig. 7d) and its derivatives containing *para*-substituents CH_3 , OH, Br, and NO_2 were oxidized to corresponding sulfoxides with 99-100% selectivity in methanolic solutions upon the action of a light diode source [105]. The composite photocatalyst $\text{CdS/C}_3\text{N}_4$ obtained by treatment of cadmium sulfide with ultrasonically-exfoliated carbon nitride was used as a photocatalyst in these systems.

Substrates containing electron-donor substituents in the benzene ring were oxidized more rapidly with 62-86% conversion after 6 h irradiation. Substrates with electron-withdrawing substituents were oxidized much less efficiently with only 6% conversion after 6 h irradiation. Data obtained in spin trap experiments suggested a mechanism similar to the scheme presented by Zhang et al. [102], who proposed activation of the substrate and oxygen molecules with the participation of both photogenerated charge carriers, namely, holes to give the radical-cation of sulfide and electrons to react with oxygen to give the superoxide anion-radical. These intermediates react with each other to give active persulfoxide. Due to the protic methanol solvent, the persulfoxide can be stabilized by hydrogen bonding, which facilitates its electrophilic attack on another substrate molecule to give two sulfoxide molecules.

TABLE 5. Photocatalytic Oxidative Coupling of Benzylamine to Give N-Benzylidenebenzylamine in Systems Derived from g- C_3N_4 Under Optimal Conditions

Photocatalyst, mg Substrate, mmole P_{O_2} , MPa Medium, ml T , °C t , h λ_{irr} , nm X , % S , % Ref.

ДМФА = DMF ТГФ = THF

Notes: X) conversion, S) selectivity, DMF) dimethylformamide, THF) tetrahydrofuran, EtOAc) ethyl acetate; light source: ^a300-W Xe lamp, ^blight diode, ^c50-W Xe lamp, ^d250-W medium-pressure Hg lamp, ^eyield, ^fmole %, ^gair pressure.

Oxidative coupling reaction

Formation of carbon–nitrogen bonds. The formation of such bonds can occur in the oxidation of amines and is a key chemical reaction in the synthesis of important products such as dyes, drugs, and pesticides. In addition to well-known thermal regimes of such reactions, there have been recent attempts to carry out these processes by the action of light, including experiments with carbon nitride as the photocatalyst (Table 5). Thus, the photocatalytic oxidative coupling of a series of benzylamines to give the corresponding imines was carried out using mpg-C₃N₄ prepared by the pyrolysis of a mixture of cyanamide and SiO₂ nanoparticles with subsequent removal of the silica matrix by treatment with NH₄HF₂ in acetonitrile solutions [106]. The complete conversion of benzylamine to give N-benzylidenebenzylamine with 99% selectivity was achieved after 3.5 h irradiation under optimal conditions in 10 ml acetonitrile, 0.6 mmole substrate, $P_{O_2} = 0.5$ MPa, $\lambda_{irr} > 420$ nm at 80°C. Benzylamines containing electron-donor substrates (CH₃ and OCH₃) are more reactive than substrates with electron-withdrawing groups (Cl and CF₃). Furthermore, the rate of conversion of *para*-substituted benzylamines is higher than for the *meta*- and *ortho*-isomers. This latter discrepancy is apparently related to steric hindrances. The oxidation of pyridylmethylamine and thiophenemethylamine proceeded much more efficiently than for their phenyl analogs. Aniline proved virtually inert under the abovementioned conditions with only 1% conversion. The oxidation of a series of secondary amines (N-benzylaniline, 1,2,3,4-tetrahydroisoquinoline, and 1,2,3,4-tetrahydroquinoline) gave high yields of the corresponding imines, while the oxidation of indoline and imidazoline gave indole and an imidazole derivative. Su et al. [6] proposed a likely mechanism for the oxidative coupling of amines with initiation of the substrate transformations involving both electrons and holes photogenerated in carbon nitride.

Su et al. [106] also used mesoporous GCN to carry out the photocatalytic synthesis of benzoxazoles, benzimidazoles, and benzothiazoles. This reaction involves the oxidative coupling of benzylamines with 2-aminophenol, 2-aminothiophenol, and *o*-phenylenediamine to give imines, which undergo intramolecular cycloaddition into the desired products (Fig. 6) in high yield after irradiation of acetonitrile solutions of the substrates for 4–5 h at 100°C.

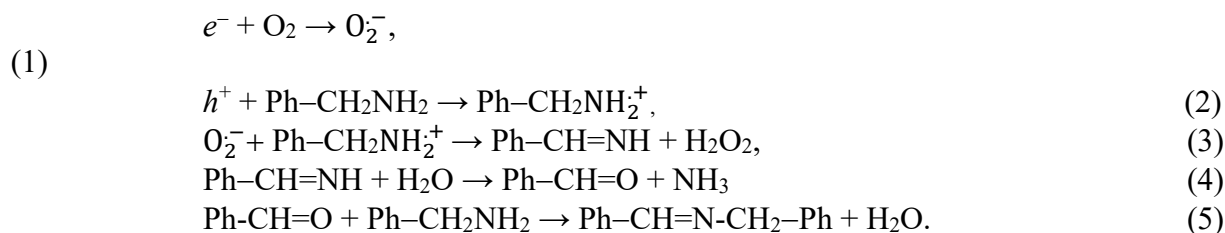
Fig. 6. Scheme for the one-step synthesis of benzoxazoles, benzimidazoles, and benzothiazoles [106].

400 nm = 400 nm

Exfoliated GCNs modified with C≡N groups showed photocatalytic properties in the oxidative coupling of benzylamine and its derivatives containing electron-donor (*p*-CH₃, *p*-CH₃O, *m*-CH₃) and electron-withdrawing groups (*p*-F, *p*-Cl, *p*-Br, *p*-Cl, *o*-Cl) to give the corresponding imines. . The photocatalysts were obtained by pyrolysis of a mixture of diacetamide with ammonium chloride [107] or a mixture of melamine and trithiocyanuric acid [108] with subsequent heat treatment in an inert atmosphere. The substrates were converted

almost completely into imines with 90-99% selectivity by the action of visible light on the reaction mixtures in acetonitrile for 4-6 h at P_{O_2} 1 atm at 20°C [107] or 60°C [108].

The higher photocatalytic activity of GCN modified with cyanide groups than for ordinary g-C₃N₄ is related to greater visible light absorption. Furthermore, the modified sample has higher adsorption capacity relative to oxygen and improved separation of photogenerated electrons (e^-) and holes (h^+), which induce the formation of the $O_2^{\cdot-}$ anion-radical from an O₂ molecule (reaction (1)) and a radical-cation from the substrate molecule (reaction (2)). Subsequent reactions of these radical species (reactions (3-5)) lead to the final products in accord with the proposed mechanism involving the formation of phenylacetaldehyde (reaction (4)) and its condensation with benzylamine (reaction (5)):



Benzylamine (Table 5), its derivatives containing electron-donor (CH₃ and CH₃O) and electron-withdrawing groups (Cl, CF₃), secondary cyclic and sulfur-containing heterocyclic amines are oxidized to the corresponding imines with 99% selectivity by the action of visible light at room temperature using mesoporous CGN modified with C=O groups. Such photocatalyst was obtained in the thermolysis of a mixture of precursors (cyanamide, dicyandiamide, and melamine) and ammonium sulfate (mpO-C₃N₄) [109]. Zhang et al. [109] attributed the higher activity of this material than for bulk CGN and unmodified mpg-C₃N₄ to the presence of carbonyl groups capable of activating oxygen and hydrogen peroxide generated *in situ*, which participates in the oxidation of the substrates.

A photocatalyst derived from nanoporous carbon nitride obtained by the pyrolysis of a mixture of dicyandiamide and thiourea with subsequent immobilization of the *tris*-bipyridyl iron(II) complex (Fe(bpy)₃)mpg-C₃N₄) proved active in the oxidative coupling of benzylamine (Table 5) and its derivatives with electron-donor (CH₃ and CH₃O) and electron-withdrawing groups (Cl, Br, and CN) [110]. This reaction proceeds with rather high efficiency in a number of solvents but, as in other studies, the greatest substrate conversion is found when using acetonitrile (Table 5). The presence of the iron complex in the photocatalyst enhances its visible light absorption and facilitates the separation of photogenerated charges due to electron transfer from the excited triplet state of the complex to the conductance band of GCN. Oxygen present in the system presumably is converted to the singlet state and reacts with benzylamine to give an intermediate peroxide, which fragments to release H₂O₂ and an intermediate that reacts with a substrate molecule to give an imine.

Singlet oxygen was the major oxidizing agent in a photocatalytic system derived from bulk GCN obtained by the pyrolysis of melamine followed by oxidative treatment with a mixture of concentrated HNO₃ and H₂SO₄ (g-C₃N₄(C=O)) [104]. The photoexcitation of this material gives mainly triplet excitons due to the existence of linked carbonyl groups which convert to the triplet state upon the action of light quanta and are capable of energy transfer to O₂ molecules, converting them to the singlet state. Using this photocatalyst, benzylamine (Table 5), its derivatives containing various substituents (*p*-F, *p*-Cl, *p*-CH₃, and *p*-CH₃O) as well as

thiophenemethylamine are converted almost quantitatively into the corresponding imines upon irradiation of their solutions in acetonitrile with the unfiltered light of a xenon lamp for 8-16 h.

Fig. 7. Probable mechanism for the photocatalytic oxidation of benzylamine (a) and aniline (b) using BiVO₄/g-C₃N₄. Reprinted with permission [88]. Copyright (2017) American Chemical Society.

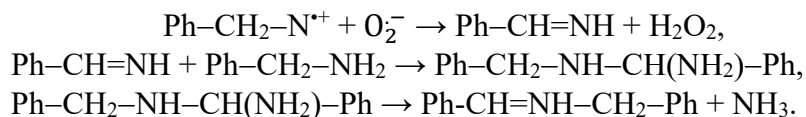
400 nm = 400 nm

The BiVO₄/g-C₃N₄ composite prepared by heating a mixture of bismuth vanadate and carbon nitride obtained by the pyrolysis of melamine and active in the oxidation of benzyl alcohol was also used for the oxidative coupling of amines [88]. With equal amounts of the components in the composite, benzylamine in acetonitrile solution is converted almost quantitatively into the imine after irradiation with visible light for 16 h at room temperature (Table 5). Benzaldehyde, which is also obtained in the oxidation of benzylamine using GCN by itself, is formed in this case at the onset of irradiation as an intermediate. A mechanism for this photocatalytic reaction was proposed on the basis of these data and other experimental results (Fig. 7a), in which the electron and hole formed after light absorption induce oxidation-reduction transformations in the system: the holes oxidize substrate molecules adsorbed on an electrophilic vanadium site along with its deprotonation and formation of a radical species (intermediate II), while the electrons are captured by oxygen molecules to give the O₂⁻ anion-radical. Then, intermediate II reacts with O₂⁻ to give intermediate III, which fragments to give benzaldehyde and intermediate IV. Then, hydroxylamine is released upon the protonation of intermediate IV, leading to the regeneration of V^V sites on the surface of BiVO₄/g-C₃N₄ and completion of the photocatalytic cycle. The final product, N-benzylidenebenzylamine, is formed as a result of the condensation of benzaldehyde and benzylamine.

Samanta et al. [88] also studied the oxidation of aniline using the BiVO₄/g-C₃N₄ composite. Under optimal conditions similar to those given in Table 5, aniline undergoes 20.2% conversion to give azobenzene and N-phenylbenzene-1,4-diamine with 82.3 and 17.7% selectivity, respectively. The likely mechanism for this reaction is given in Fig. 7b. In the presence of sole GCN the product of the oxidation of aniline (*X* = 11.5%) under these conditions was predominantly azobenzene (*S* = 94.8%). At the same time, the photocatalytic oxidation of mixtures of benzyl alcohol with benzylamine and of benzyl alcohol with aniline using BiVO₄/g-C₄N₄ gave N-benzylidenebenzylamine (*S* = 76.4%) and azobenzene (*S* = 71.2%) as the major products, which, according to Samanta et al. [88], is in accord with the proposed mechanistic schemes for these reactions (Fig. 7b).

Benzylamine, its derivatives with electron-donor (*p*-CH₃, *o*-CH₃, *p*-CH₃O) and electron-withdrawing substituents (*p*-F, *p*-Cl, *p*-CF₃) as well as phenyl-β-ethylamine and furan-2-methylamine were oxidized using a hybrid composite photocatalyst CdS/C₃N₄ with core-shell structure obtained by the deposition of g-C₃N₄ nanosheets synthesized by the combined thermal condensation of dicyandiamide and barbituric acid on CdS nanowires [111]. The energy structure of the heterojunction interface between the composite components facilitates the separation of the photogenerated charges and enhanced activity in comparison with the individual components due to a favorable matching of their band gaps. Under optimal

conditions, benzylamine is converted quantitatively to N-benzylidenebenzylamine (Table 5). When the benzene ring has substituents capable of steric hindrance, the conversion of benzylamines is lower although the selectivity in all cases is >99%. The proposed mechanism entails with the participation of photogenerated electrons and holes, which react with oxygen molecules (reaction (1)) and the substrate (reaction (2)), respectively, to give intermediates that undergo a series of transformations leading to the final products:



The hydrogen peroxide formed in this reaction also participates in the oxidation of the substrates. The reaction proceeds more rapidly when hydrogen peroxide is used instead of oxygen. The aerobic oxidative amidation of aromatic aldehydes by amines upon irradiation of the reaction mixtures in tetrahydrofuran with visible light is achieved in high yield using a nanocomposite derived from GCN prepared by a solvothermal method from melamine and cyanuric chloride and deposition of silver nanoparticles onto its surface (Fig. 8) [112]. The substrates used were benzaldehyde, its derivatives containing Br, Cl, F, NO₂, CF₃, CH₃O, and CH₃ groups in the *para* position or Br, F, NO₂, and CF₃ in the *meta* position, dichloro-substituted benzaldehyde, β- and α-naphthaldehydes, a series of heteroaromatic aldehydes as well as various amines, namely, pyrrolidine, morpholine, and piperidine. The mechanism for this reaction involving Ag/g-C₃N₄ assumes the formation of an intermediate enamine from the aldehyde and amine, photocatalytic oxidation of the tetrahydrofuran solvent to give its hydroperoxide, which oxidizes the enamine intermediate with formation of the final product.

Fig. 8. Scheme for the photocatalytic amidation of aromatic aldehydes by amines using mesoporous carbon nitride [112].

Fig. 9. Scheme for the photocatalytic oxidative coupling of N-aryltetrahydroisoquinolines with nucleophiles (NuH) induced by mesoporous carbon nitride [115].

A thioamide bond is formed in the Willgerodt-Kindler reaction of amines and elemental sulfur as the oxidizing agent in the presence of potassium polyheptazinimide [113]. Substituted benzylamines react with heterocyclic and aliphatic methylamines to give thioamides in 68-92% yield upon irradiation with a light diode at 461 nm at 70°C for 20 h.

Formation of carbon-carbon bonds. The photocatalytic synthesis of benzoin is accomplished in the aerobic oxidation of benzyl alcohol via the C-C coupling between benzaldehyde molecules forming as an intermediate in the presence of potassium-doped GCN, obtained by its treatment with aqueous KOH [114]. The efficiency of this reaction is due to modification of the electronic structure and chemical properties of the GCN surface upon alkaline treatment. The intercalation of K⁺ ions into the g-C₃N₄ structure enhances light absorption and separation of photogenerated charge carriers. Furthermore, alkaline treatment

favors to the efficient deprotonation of the surface amino groups of GCN, which enhances nucleophilicity and significantly increases the rate of the C–C coupling reaction between the benzaldehyde molecules.

The photocatalytic oxidative C–C bond coupling in the reaction of tertiary amines (various N-aryltetrahydroisoquinolines) with a series of nucleophilic reagents (substituted nitroalkanes and malonates) was carried out using mesoporous GCN (Mannich reaction (Fig. 9)) [115].

Fig. 10. Mechanistic scheme for the photocatalytic formation of 1,3,4-oxadiazoles [117].

Fig. 11. Scheme for the photocatalytic oxidative coupling of resveratrol and δ -vinipherine [118] (a) and the cycloaddition of *trans*-anethole with 2,3-dimethyl-1,3-butadiene in the presence of carbon nitride [119] (b).

400 nm = 400 nm

The desired products were obtained in 85-92% yield in the case of nitroalkanes and 65-84% yield in the case of malonates upon irradiation in the presence of oxygen using visible light from a 60-W household lamp for 22-34 h. When using N-phenyl-1,2,3,4-tetrahydroisoquinoline and proline as the cocatalyst, C-C coupling was achieved with acetone both as the nucleophile and solvent with 94% yield of the desired product. In the case of weaker nucleophilic agents such as allylstannanes, allylsilanes, and allylboranes in the presence of mpg-C₃N₄, the photocatalytic oxidative allylation of a series of tetrahydroisoquinolines was carried out in the air in the presence of mpg-C₃N₄ [116]. The desired products were obtained in 71-96% yield upon the action of visible light in methanolic solutions at room temperature.

Oxidative cyclization

The photocatalytic synthesis of twelve 1,3,4-oxadiazoles with aryl, heteroaryl, and alkyl substituents in 84-18% yields was achieved by the oxidative cyclization of the corresponding N-acylhydrazones using potassium polyheptazinimide (K-PHI) obtained by annealing a mixture of 5-aminotetrazole with potassium and lithium chlorides at 550°C. The reaction proceeded at 80°C in acetonitrile solutions upon irradiation with a light diode (461 nm) in the presence of elemental sulfur, a milder acceptor of photogenerated electrons than oxygen (Fig. 10).

The mechanism shown in Fig. 10 anticipates the substrate transformations with the participation of both charge carriers photogenerated in K-PHI, namely, holes (h^+), which oxidize the N-acylhydrazone to give a radical-cation, and electrons (e^-), which are captured by sulfur to give the S₈^{•-} anion-radical. Further reactions of these intermediate radical species through steps entailing bound proton-electron transfers involving S₈^{•-} and the resultant hydrosulfide anion (HS₈⁻) lead to an oxadiazole and H₂S₈.

Mesoporous GCN was used for the aerobic oxidative coupling of 4-hydroxy-*trans*-stilbenes to give δ -vinipherine and its analogs, which serve as valuable pharmaceutical precursors (Fig. 11a) [118]. The irradiation of air-saturated reaction mixtures in

acetonitrile at room temperature with a light diode source (410 nm) gives the desired products in a rather high yield.

The photocatalytic Diels-Alder reaction between *trans*-anethole and a series of dienes was carried out under aerobic conditions using g-C₃N₄ with irradiation by light with $\lambda > 420$ nm (Fig. 11b) [119]. This reaction proceeds very efficiently in nitromethane; the quantum yield reaches 47% for the model reaction of *trans*-anethole with 2,3-dimethyl-1,3-butadiene. Nineteen products were obtained in moderate (38-54%) and high yield (74-98%) using various olefins. The mechanism proposed assumed the participation of both photogenerated charge carriers, namely, electrons, which are captured by oxygen to give the anion-radical species that serve in electron transfer, and holes, which accept electrons from *trans*-anethole to give its radical-cation. In subsequent steps, vinylcyclobutane is formed as an intermediate, which rearranges to give the final product.

Conclusion

In summarizing our examination of the photocatalytic transformations of various classes of organic compounds, we note that GCN is a unique semiconductor photocatalyst displaying relatively high activity, selectivity, sensitivity to visible light, chemical and photochemical stability. This material offers extremely broad possibilities for tuning the energy parameters of the photogenerated charge carriers and the morphology and reactivity of the photocatalyst surface.

GCN clearly displays its dual nature in these reactions. On one hand, similar to classical inorganic semiconductor photocatalysts, the vast majority of transformations with GCN systems are achieved with the participation of a limited number of photogenerated intermediates, namely, electrons of the conductance band and oxygen radical-cations as well as holes of the valence band and hydroxyl radicals. On the other hand, due to the selective van der Waals interaction of the GCN framework with aromatic substrates and of the functional groups of GCN with the corresponding functional groups of the substrates, this photocatalyst possesses unique possibilities for carrying out selective processes. The design of photocatalysts derived from GCN combines both molecular engineering entailing the introduction of dopant atoms, additional aromatic fragments, and functional groups into GCN as well as solid state engineering previously tested on inorganic semiconductors. Among the latter are the formation of mesoporous materials with a well-developed active surface, the transition to nanodimensional crystals, modification of the surface by cocatalysts including electron and hole acceptors, the association of GCN with molecular or semiconductor sensitizers, and the combination of GCN with other semiconductors to give heterostructures with suitable band gap arrangement. Similar to extensively studied layered dichalcogenides of transition metals, GCN can be subjected to exfoliation to give layered species with nanodimensional thickness, even monoatomic layers, whose reactivity and selectivity in important industrial organic reactions have still not been properly characterized and interpreted.

Reactions proceeding under mild conditions without thermal activation and with the participation of molecular oxygen similar to reactions in biological systems are especially interesting among reported oxidative photocatalytic transformations of organic compounds using GCN. Reactions giving products with added value (biologically active and optically active molecules) as well as coupled reactions, in which the selective oxidation of the substrate is accompanied by storage of light energy as molecular oxygen, are especially interesting from a practical viewpoint. We may expect that the reported examples of selectivity in organic

photocatalytic reactions by layered carbon nitride will stimulate the search for promising new reactions. As an example, we note the synthesis of carboxylic acids similar to the Kolbe reaction, which might be possible due to the high activity of GCN as a photocatalyst for the conversion of CO₂ [8, 20-23, 27-30].

On the whole, GCN significantly expands the range of photocatalytic processes considered traditional for inorganic semiconductors, combining both the most promising characteristics of molecular and metal complex photocatalysts, including the feasibility of varying their properties and complementary structures of the photocatalyst and substrate, as well as crystalline semiconductors (collective nature of the electronic properties and delocalization of the photogenerated charges, stability, and high light sensitivity). In the future, the availability of GCN allows us to expect that this material will find broad applications in complex photocatalytic systems as 2D platforms, whose surface can carry nanoparticles of other semiconductors and metals, metal complex cocatalysts and sensitizers as well as pores of a specific size and functional groups with required properties combining all these components into a single photochemically active ensemble.

REFERENCES

1. X. Wang, K. Maeda, A. Thomas, et al., *Nat. Mater.*, **8**, No. 1, 76-80 (2009).
2. X. Chen, Y. S. Jun, K. Takanabe, et al., *Chem. Mater.*, **21**, No. 18, 4093-4095 (2009).
3. X. Wang, Maeda, X. Chen, et al., *J. Am. Chem. Soc.*, **131**, No. 5, 1680-1681 (2009).
4. K. Maeda, X. Wang, Y. Nishihara, et al., *J. Phys. Chem. C*, **113**, No. 12, 4940-4947 (2009).
5. A. Thomas, A. Fischer, F. Goettmann, et al., *J. Mater. Chem.*, **18**, No. 41, 4893-4908 (2008).
6. J. Zhu, P. Xiao, and S. A. C. Carabineiro, *ACS Appl. Mater. Interfaces*, **6**, No. 19, 16449-16465 (2014).
7. Yuyang Kang, Yongqiang Yang, Li-Chang Yin, et al., *Adv. Mater.*, **27**, No. 31, 4572-4577 (2015).
8. Jiuqing Wen, Jun Xie, Xiaobo Chen, and Xin Li, *Appl. Surf. Sci.*, **391**, 72-123 (2017).
9. A. A. Stroyuk, A. E. Raevskaya, and S. Ya. Kuchmy, *Teor. Éksperim. Khim.*, **54**, No. 1, 3-32 (2018) [*Theor. Experim. Chem.*, **54**, No. 1, 1-35 (2018)].
10. X. Wang, S. Blechert, and M. Antonietti, *ACS Catal.*, **2**, No. 8, 1596-1606 (2012).
11. J. Liu, H. Wang, and M. Antonietti, *Chem. Soc. Rev.*, **45**, No. 8, 2308-2326 (2016).
12. D. Huang, X. Yan, M. Yan, et al., *ACS Appl. Mater. Interfaces*, **10**, No. 25, 21035-21055 (2018).
13. J. Zhang, Y. Chen, and X. Wang, *Energy and Environmental Sci.*, **8**, No. 11, 3092-3108 (2015).
14. T. S. Miller, A. B. Jorge, T. M. Suter, et al., *Phys. Chem. Chem. Phys.*, **19**, No. 24, 15613-15638 (2017).
15. I. F. Teixeira, E. C. M. Barbosa, S. C. E. Tsang, and P. H. C. Camargo, *Chem. Soc. Rev.*, **47**, No. 20, 7783-7817 (2018).
16. W. Iqbal, B. Yang, X. Zhao, et al., *Catal. Sci. and Technol.*, **8**, No. 18, 4576-4599 (2018).
17. Z. Wang, X. Hu, G. Zou, et al., *Sustain. Energy and Fuels*, **3**, No. 3, 611-655 (2019).
18. L. Lin, Z. Yu, and X. Wang, *Angew. Chem. Int. Ed.*, **58**, No. 19, 6164-6175 (2019).
19. N. Tian, H. Huang, X. Du, *J. Mater. Chem. A*, **7**, No. 19, 11584-11612 (2019).

20. Yun Zheng, Lihua Lin, Bo Wang, and Xinchun Wang, *Angew. Chem. Int. Ed.*, **54**, No. 44, 12868-12884 (2015).
21. Wee-Jun Ong, Lling-Lling Tan, Yun Hau Ng, et al., *Chem. Rev.*, **116**, No. 12, 7159-7329 (2016).
22. Junwei Fu, Jiaguo Yu, Chuanjia Jiang, and Bei Cheng, *Adv. Energy Mater.*, **8**, No. 3, 1701503 (2017).
23. S. Cao, J. Low, J. Yu, and M. Jaroniec, *Adv. Mater.*, **27**, No. 13, 2150-2176 (2015).
24. X. Li, A. F. Masters, and T. Maschmeyer, *Chem. Commun.*, **53**, No. 54, 7438-7446 (2017).
25. P. Kumar, R. Boukherroub, and K. Shankar, *J. Mater. Chem. A*, **6**, No. 27, 12876-12931 (2018).
26. M. Volokh, G. Peng, J. Barrio, and M. Shalom, *Angew. Chem. Int. Ed.*, **58**, No. 19, 6138-6151 (2019).
27. Chunling Wang, Zhuxing Sun, Ying Zheng, and Yun Hang Hu, *J. Mater. Chem. A*, **7**, No. 3, 865-887 (2019).
28. A. L. Stroyuk and S. Ya. Kuchmy, *Teor. Éksperim. Khim.*, **53**, No. 6, 337-360 (2017) [*Theor. Experim. Chem.*, **53**, No. 6, 359-386 (2017)].
29. M. Shen, L. Zhang, and J. Shi, *Nanotechnology*, **29**, 412001 (2018).
30. Z. Sun, N. Talreja, H. Tao, et al., *Angew. Chem. Int. Ed.*, **57**, No. 26, 7610-7627 (2018).
31. Y. Chen, G. Jia, Y. Hu, et al., *Sustain. Energy and Fuels*, **1**, No. 9, 1875-1898 (2017).
32. Y. Fang and X. Wang, *Chem. Commun.*, **54**, No. 45, 5674-5687 (2018).
33. Yuqing Luo, Yan Yan, Shasha Zhang, et al., *J. Mater. Chem. A*, **7**, No. 3, 901-924 (2019).
34. J. Safaei, N. A. Mohamed, M. F. M. Noh, et al., *J. Mater. Chem. A*, **6**, No. 45, 22346-22380 (2018).
35. W. Niu and Y. Yang, *ACS Energy Lett.*, **3**, No. 11, 2796-2815 (2018).
36. M. M. Xavier, P. R. Nair, and S. Mathew, *Analyst*, **144**, No. 5, 1475-1491 (2019).
37. F. Parrino, M. Bellardita, E. I. García-López, et al., *ACS Catal.*, **8**, No. 12, 11191-11225 (2018).
38. Y. Wang, X. Wang, and M. Antonietti, *Angew. Chem. Int. Ed.*, **57**, No. 49, 15936-15947 (2012).
39. Jun Chen, Jie Cen, Xiaoliang Xu, and Xiaonian Li, *Catal. Sci. and Technol.*, **6**, No. 2, 349-362 (2018).
40. A. Savateev, I. Ghosh, B. König, and M. Antonietti, *Angew. Chem. Int. Ed.*, **57**, No. 49, 15936-15947 (2018).
41. G. Marci, E. I. García-López, and L. Palmisano, *Catal. Today*, **315**, 126-137 (2018).
42. A. Savateev and M. Antonietti, *ACS Catal.*, **8**, No. 10, 9790-9808 (2018).
43. Z. Zhao, Y. Suna, and F. Dong, *Nanoscale*, **7**, No. 1, 15-37 (2015).
44. K. S. Lakhi, D.-H. Park, and K. Al-Bahily, *Chem. Soc. Rev.*, **46**, No. 1, 72-101 (2017).
45. O. Stroyuk, *Solar Light Harvesting with Nanocrystalline Semiconductors, Lecture Notes in Chemistry Series*, Springer (2017).
46. G. Mamba and A. K. Mishra, *Appl. Catal. B*, **198**, 347-377 (2016).
47. W. J. Ong, *Front. Mater.*, **4**, No. 11, 1-10 (2017).
48. X. Dong and F. Cheng, *J. Mater. Chem. A*, **3**, No. 47, 23642-23652 (2015).
49. Z. Zhou, Y. Zhang, Y. Shen, et al., *Chem. Soc. Rev.*, **47**, No. 7, 2298-2321 (2018).
50. Q. Weng, G. Li, X. Feng, et al., *Adv. Mater.*, **30**, 1801600 (2018).

51. G. Liu, C. Zhen, Y. Kang, et al., *Chem. Soc. Rev.*, **47**, No. 16, 6410-6444 (2018).
52. Yuan Li, Jun Li, and Gaoke Zhang, *ACS Sustain. Chem. and Eng.*, **7**, No. 4, 4328-4389 (2019).
53. M. Ilkaeva, L. Krivtsov, E. Bartashevich, et al., *Green Chem.*, **19**, No. 18, 4299-4304 (2017).
54. Wenting Wu, Jinqiang Zhang, Weiyu Fan, et al., *ACS Catal.*, **6**, No. 5, 3365-3371 (2016).
55. P. Zhang, Y. Wang, J. Yao, et al., *Adv. Synth. Catal.*, **353**, No. 9, 1447-1451 (2011).
56. S. Verma, R. B. Nasir Baig, M. N. Nadagouda, and R. S. Varma, *Catal. Today*, **309**, 248-252 (2018).
57. W. Zhang, A. Bariotaki, I. Smonou, and F. Hollmann, *Green Chem.*, **19**, No. 9, 2096-2100 (2017).
58. S. Verma, R. B. Nasir Baig, M. N. Nadagouda, and R. S. Varma, *ACS Sustain. Chem. and Eng.*, **4**, No. 4, 2333-2336 (2016).
59. S. Samanta and R. Srivastava, *Appl. Catal. B*, **218**, 621-636 (2017).
60. Juan Liu, Yanmei Yang, Naiyun Liu, et al., *Green Chem.*, **16**, No. 10, 4559-4565 (2014).
61. Yalin Zhang, Lulu Hu, Cheng Zhu, et al., *RCS Adv.*, **6**, No. 659, 60394-60399 (2016).
62. Yalin Zhang, Lulu Hu, Cheng Zhu, et al., *Catal. Sci. and Technol.*, **6**, No. 19, 7252-7258 (2016).
63. Pengfei Zhang, Haoran Li, and Yong Wang, *Chem. Commun.*, **50**, No. 48, 6312-6315 (2014).
64. A. Savateev, B. Kurpil, A. Mishchenko, et al., *Chem. Sci.*, **9**, No. 14, 3584-3591 (2018).
65. X. Chen, J. Zhang, X. Fu, et al., *J. Am. Chem. Soc.*, **131**, No. 33, 11658-11659 (2009).
66. Z. Ding, X. Chen, M. Antonietti, and X. Wang, *ChemSusChem*, **4**, No. 2, 274-281 (2010).
67. Xiangju Ye, Yanjuan Cui, Xiaoqing Qiu, and Xinchun Wang, *Appl. Catal. B*, **152/153**, 383-389 (2014).
68. S. M. Hosseini, M. Ghiaci, S. A. Kulinich, W. Wunderlich, et al., *J. Phys. Chem. C*, **122**, No. 48, 27477-27485 (2018).
69. Bishal Bhuyan, Meghali Devi, Debashree Bora, et al., *Eur. J. Inorg. Chem.*, No. 34, 3849-3858 (2018).
70. Xiangju Ye, Yun Zheng, and Xinchun Wang, *Chin. J. Chem.*, **32**, No. 6, 498-506 (2014).
71. B. Long, Z. Ding, and X. Wang, *ChemSusChem*, **6**, No. 11, 2074-2078 (2013).
72. F. Su, S. C. Mathew, G. Lipner, et al., *J. Am. Chem. Soc.*, **132**, No. 46, 16299-16301 (2010).
73. Fei Li, Yong Wang, Jian Du, et al., *Appl. Catal. B*, **225**, 258-263 (2018).
74. Pengfei Zhang, Jiang Deng, Jianyong Mao, et al., *Chin. J. Catal.*, **36**, No. 9, 1580-1586 (2015).
75. L. Zhang, D. Liu, J. Guan, et al., *Mater. Res. Bull.*, **59**, 84-92 (2014).
76. M. Lima, A. M. T. Silva, C. G. Silva, and J. L. Faria, *J. Catal.*, **353**, 44-53 (2017).
77. Min Zhou, Pengju Yang, Rusheng Yuan, et al., *ChemSusChem*, **10**, No. 22, 4451-4456 (2017).
78. Jing Ding, Wei Xu, Hui Wan, et al., *Appl. Catal. B*, **221**, 626-634 (2018).
79. M. Bellardita, E. I. García-López, G. Marci, et al., *Appl. Catal. B*, **220**, 222-233 (2018).
80. Y. Chen, J. Zhang, M. Zhang, and X. Wang, *Chem. Sci.*, **4**, No. 8, 3244-3248 (2013).
81. M. Ilkaeva, I. Krivtsov, J. R. García, et al., *Catal. Today*, **315**, 138-148 (2018).
82. G. Marci, E. I. García-López, F. R. Pomilla, et al., *Catal. Today*, **328**, 21-28 (2019).
83. A. Savateev, D. Dontsova, R. Kurpil, and M. Antonietti, *J. Catal.*, **350**, 203-211 (2017).

84. Z. Zheng and X. Zhou, *Chin. J. Chem.*, **30**, No. 8, 1683-1686 (2012).
85. S. Verma, R. B. Nasir Baig, M. N. Nadagouda, and R. S. Varma, *ACS Sustain. Chem. and Eng.*, **4**, No. 3, 1094-1098 (2016).
86. M. J. Lima, P. B. Tavares, A. M. T. Silva, et al., *Catal. Today*, **287**, 70-77 (2017).
87. P. V. R. K. Ramacharyulu, S. J. Abbas, S. R. Sahoo, and S. C. Ke, *Catal. Sci. and Technol.*, **8**, No. 11, 2825-2834 (2018).
88. S. Samanta, S. Khilari, D. Prodhon, and R. Srivastava, et al., *ACS Sustain. Chem. and Eng.*, **5**, No. 3, 2562-2577 (2017).
89. X. Dai, M. Xie, S. Meng, et al., *Appl. Catal. B*, **158/159**, 382-390 (2014).
90. H. Kasap, C. A. Caputo, B. C. M. Martindale, et al., *J. Am. Chem. Soc.*, **138**, No. 29, 9183-9192 (2016).
91. Hui Wang, Xianshun Sun, Dandan Li, et al., *J. Am. Chem. Soc.*, **139**, No. 6, 2468-2473 (2017).
92. K. Cerdan, W. Ouyang, J. C. Colmenares, *Chem. Eng. Sci.*, **194**, 78-84 (2019).
93. A. Kumar, P. Pawan Kumar, A. Kumar Pathak, et al., *Chem. Select.*, **2**, No. 12, 3437-3443 (2017).
94. L. Song, S. Zhang, X. Wu, et al., *Ind. and Eng. Chem. Res.*, **51**, No. 28, 9510-9514 (2012).
95. Jinjuan Xue, Xinyao Li, Shuaishuai Ma, et al., *J. Mater. Sci.*, **54**, No. 1275-1290 (2019).
96. Jie Xu, Liufeng Luo, Guangrui Xiao, et al., *ACS Catal.*, **4**, No. 9, 3302-3306 (2014).
97. I. Krivtsov, E. I. García-López, G. Marci, et al., *Appl. Catal. B*, **204**, 430-439 (2017).
98. Qi Wu, Yiming He, Huili Zhang, et al., *Mol. Catal.*, **436**, 10-18 (2017).
99. M. Ilkaeva, I. Krivtsov, E. I. García-López, et al., *J. Catal.*, **359**, 212-222 (2018).
100. Huili Zhang, Zhiyuan Feng, Yekun Zhu, et al., *J. Photochem. and Photobiol.*, **371**, 1-9 (2019).
101. S. Xu, P. Zhou, Z. Zhang, et al., *J. Am. Chem. Soc.*, **139**, No. 41, 14775-14782 (2017).
102. P. Zhang, Y. Wang, H. Li, and M. Antonietti, *Green Chem.*, **14**, No. 7, 1904-1908 (2012).
103. Yunfeng Zhu, Xiaoyan Li, and Mingyuan Zhu, *Catal. Sci. and Technol.*, **85**, 5-8 (2016).
104. H. Wang, S. Jiang, S. Chen, et al., *Adv. Mater.*, **28**, No. 32, 6940-6945 (2016).
105. Yong Xu, Zi-Cheng Fu, Shuang Cao, et al., *Catal. Sci. and Technol.*, **7**, No. 3, 587-595 (2017).
106. F. Su, S. C. Mathew, L. Möhlmann, et al., *Angew. Chem. Int. Ed.*, **50**, No. 3, 657-660 (2011).
107. Di Zhang, Xinghua Han, Ting Dong, et al., *J. Catal.*, **366**, 237-244 (2018).
108. Hao Tan, Xianmo Gu, Peng Kong, et al., *Appl. Catal. B*, **242**, 67-75 (2019).
109. Jun-Jun Zhang, Jie-Min Ge, Hong-Hui Wang, et al., *ChemCatChem*, **8**, No. 22, 3441-3445 (2016).
110. A. Kumar, P. Kumar, Ch. Josi, et al., *Green Chem.*, **18**, No. 8, 2514-2521 (2016).
111. Yong Xu, Yong Chen, and Wen-Fu, *Appl. Catal. B*, **236**, 176-183 (2018).
112. Lingling Wang, Min Yu, Chaolong Wu, et al., *Adv. Synth. and Catal.*, **358**, No. 16, 2631-2641 (2016).
113. B. Kurpil, B. Kumru, T. Heil, et al., *Green Chem.*, **20**, No. 4, 838-842 (2018).
114. Xiang Sun, Dong Jiang, Ling Zhang, and Wenzhong Wang, *Appl. Catal. B*, **220**, 553-560 (2018).

115. L. Möhlmann, M. Baar, J. Rieß, et al., *Adv. Synth. and Catal.*, **354**, No. 10, 1909-1913 (2012).
116. L. Möhlmann and S. Blechert, *Adv. Synth. and Catal.*, **356**, No. 13, 2825-2829 (2014).
117. B. Kupril, K. Otte, M. Antonietti, and A. Savateev, *Appl. Catal. B*, **228**, 97-102 (2018).
118. T. Song, B. Zhou, G.-W. Peng, et al., *Chem. Eur. J.*, **20**, No. 3, 678-682 (2014).
119. Y. Zhao and M. Antonietti, *Angew. Chem. Int. Ed.*, **56**, No. 32, 9336-9340 (2017).